

Conservative N cycling despite high atmospheric deposition in early successional African tropical lowland forests

Isaac Ahanamungu Makelele (✉ isaacmakelele1@gmail.com)

Université Officielle de Bukavu: Universite Officielle de Bukavu <https://orcid.org/0000-0002-6768-1264>

Marijn Bauters

Kris Verheyen

Matti Barthel

Johan Six

Tobias Rütting

Samuel Bodé

Landry Cizungu Ntaboba

Basile Mujinya Bazirake

Boyemba Bosela

Fabrice Kimbesa

Corneille Ewango

Pascal Boeckx

Research Article

Keywords: Congo basin, nitrogen cycle, secondary succession, tropical forests biogeochemistry

Posted Date: March 11th, 2022

DOI: <https://doi.org/10.21203/rs.3.rs-1422824/v1>

License:   This work is licensed under a Creative Commons Attribution 4.0 International License.

[Read Full License](#)

Abstract

Background

Across the tropics, the share of secondary versus primary forests is strongly increasing. The high rate of biomass accumulation during this secondary succession relies on the availability of essential nutrients, such as nitrogen (N). Nitrogen primarily limits many young secondary forests in the tropics. However, recent studies have shown that forests of the Congo basin are subject to high inputs of atmospheric N deposition, potentially alleviating this N limitation in early succession.

Methods

To address this hypothesis, we assessed the N status along a successional gradient of secondary forests in the Congo basin. In a set-up of 18 plots implemented along six successional stages, we quantified year-round N deposition, N leaching, N₂O emission and the N flux of litterfall and fine root assimilation. Additionally, we determined the N content and C:N stoichiometry for canopy leaves, fine roots, and litter, as well as $\delta^{15}\text{N}$ of canopy leaves.

Results

We confirmed that these forests receive high amounts of atmospheric N deposition, with an increasing deposition as forest succession proceeds. Additionally, we noted lower C:N ratios, and higher N leaching losses, N₂O emission, and foliar $\delta^{15}\text{N}$ in older secondary forest (60 years). In contrast, higher foliar, litter and root C:N ratios, and lower foliar $\delta^{15}\text{N}$, N leaching, and N₂O emission in young (< 20 years) secondary forest were observed.

Conclusions

Altogether, we show that despite high N deposition, this early forest succession still shows conservative N cycling characteristics, which are likely indicating N limitation early on in secondary forest succession.

Introduction

The Democratic Republic of the Congo is home to more than 60% of the Congo basin's forest, representing the second largest contiguous block of tropical forest on the planet (de Wasseige et al. 2012). These forests are important for hosting biodiversity (Slik *et al.* 2015), and play an important role in the global carbon cycle. In particular, the carbon sink of the intact mature African forests has shown to be stable over the past decades (Hubau et al. 2020). However, these forests and the ecosystem services they provide are subject to increasing deforestation. With an ongoing population expansion in Central Africa (Gerland et al. 2014), shifting cultivation will continue to decrease the extent of pristine forests and increasingly convert it to secondary forests in the next decades (Curtis et al. 2018; Tyukavina et al. 2018). In general, secondary tropical forests exhibit high rates of biomass accumulation (Martin et al. 2013;

Poorter et al. 2016), but this productivity shows regional variation and peaks in the young central African forests (7.6 Mg above-ground biomass $\text{ha}^{-1} \text{yr}^{-1}$, Suarez et al. 2019). This high productivity is sustained by a high uptake of essential nutrients, especially early on during the secondary succession (Mcgrath et al. 2001). Nitrogen (N) limits primary production of at least 18% of terrestrial ecosystems (Du et al. 2020) and N limitation may reduce the projected increase in terrestrial C uptake due to increasing CO_2 fertilization by 24% (Meyerholt et al. 2020). Furthermore, it is well known from the Neotropics that N limitation is also pervasive in many young secondary forests (Davidson et al. 2007; Batterman et al. 2013). As such, assessing shifts in nutrient cycling underlying carbon accumulation along secondary forest succession, is vital to understand potential thresholds in the recovery of these ecosystems (Townsend et al. 2011; Sullivan et al. 2019). In practice, studies on N recuperation in tropical regions are scarce and geographically biased. Most of the research has focused on Neotropical and Southeast Asian forests, while African forests received less research attention (Bauters et al. 2018, 2019). Furthermore, existing studies focus only on either soils or plants and rarely take a whole ecosystem approach (Davidson et al. 2007; Winbourne et al. 2018; Figueiredo et al. 2019; Sullivan et al. 2019). The balance between the N inputs, outputs and plant demand ultimately determines the forest N cycle (Vitousek et al. 1986) and earlier work has shown that the N cycling properties of forests can be recovered during secondary succession, i.e. that secondary forests progressively shift from a conservative N cycle in to a more open N cycle in old growth forest (Davidson et al. 2007; Sullivan et al. 2019).

Nitrogen enters natural terrestrial ecosystems via three main pathways: mineral weathering, biological N fixation (BNF), and atmospheric deposition. On highly weathered tropical soils, the contribution of N derived from mineral weathering is minor (Vitousek et al. 1986; Porder et al. 2005). BNF represents an important source of ecosystem N and was used as the dominant argument to explain N richness of tropical forests (Jenny 1950). However, BNF is an energetically expensive process, which can be alternatively activated or downregulated by N-fixing species in response to the ecosystem N status (Hedin et al. 2009; Barron et al. 2011). As such, BNF rates are generally high in the young successional stages where N demand is high relative to N availability (Barron et al. 2011; Batterman et al. 2013; Bauters et al. 2016). Additionally, central African forest ecosystems are subjected to substantial N loads through atmospheric N deposition as NO_3^- (14.3 $\text{kg ha}^{-1} \text{yr}^{-1}$), NH_4^+ (12.2 $\text{kg ha}^{-1} \text{yr}^{-1}$) and dissolved organic N (DON, 26.6 $\text{kg ha}^{-1} \text{yr}^{-1}$) species (Bauters et al. 2019). DON represents an important constituent of total dissolved N (TDN) but is rarely quantified (Bauters et al. 2018, 2019; Van Langenhove et al. 2020). In the Congo basin, atmospheric N deposition is mostly due to biomass burning (Bauters et al. 2018). Additionally, the forest's canopy structure acts as a trap for atmospheric N particles, in a way that canopies that are more complex can lead to higher dry deposition inputs to the forest floor (Bauters et al. 2021a)

Nitrogen is removed from forest ecosystems through biomass export (e.g. logging), gaseous emissions (NO_x , N_2O and N_2), biomass burning, as well as dissolved inorganic N (DIN), organic N (DON) and particulate organic N by means of leaching and subsequent river export (Davidson and Martinelli 2009; Powers and Marín-Spiotta 2017). The soil microbial activity regulates - via mineralization and

(de)nitrification - the amount of gaseous N emission and N bioavailability. Consequently, gross rates of mineralization and (de)nitrification can affect, at least indirectly, the rate of forest regrowth (Schmidt et al. 2007). Quantification of gaseous N emissions and leaching losses of bioavailable N species are commonly used to describe recuperation of open N cycles in late successional stages (Davidson et al. 2007; Hedin et al. 2009; Figueiredo et al. 2019).

In recent years, our understanding of N cycling in the central Congo basin has increased substantially (Bauters et al. 2016, 2018; Baumgartner et al. 2020; Gallarotti et al. 2021). From these studies we know that the forests of the Congo basin receive high atmospheric N deposition (Bauters et al. 2018) but, at the same time, show relatively low rates of N₂O emission (Gallarotti et al. 2021). Especially the high N deposition loads further question if the N cycle also evolves from a conservative to a more open cycle as forest succession proceeds, as it is the case in the Neotropics (Davidson et al. 2007; Figueiredo et al. 2019). To address this, we quantified N cycle metrics along a secondary successional gradient of Afrotropical lowland forests. Particularly, we aimed to quantify the effect of secondary succession stage on N deposition, N leaching, N emission and biomass N pools and -fluxes to identify recuperation from a conservative (in young secondary forests) to an open of N cycle (in old secondary forests). For this, we set up long-term monitoring sites, comprised of 18 plots in total, implemented in triplicate along six successional stages.

Material And Methods

Study area

The study was conducted in post-agricultural forests at different successional stages within and around the Yoko Forest Reserve. The Yoko Forest Reserve (N00°17'; E25°18'; mean elevation 435 m a.s.l.) is located approximately 29 to 39 km southeast of Kisangani in DR Congo (Fig. 1). The vegetation of the region is semi-deciduous rainforest and the climate falls within the AF type in the classification of Köppen. The annual rainfall volume ranges between 1418 mm and 1915 mm and the annual mean temperature is 24.2°C (De Ridder et al. 2014). We collected the samples in a setup of 18, 40 by 40 m plots, which were set up along a secondary succession gradient that consists of six successional stages, i.e., three plots per successional stage, beginning with agricultural fields (AG) and ending with an old growth forest (OG). The AG sites consisted of cassava fields that were prepared (e.g., the forest on the site was cleared and burned) in May 2018 and planted in July 2018. The secondary forests were aged 5, 12, 20 and 60 years-old. Soils in the region are highly weathered Ferrasols, being poor in nutrients, with low pH and dominated by a sandy texture (Table 1).

Table 1

Vegetation structure and soil characteristics of the plots at the study site. Basal area (BA), aboveground biomass (AGB), bulk density (BD) and soil organic carbon (SOC) are, respectively, basal area, aboveground biomass, soil bulk density and soil organic carbon. AG, 5yrs, 12yrs, 20yrs, 60yrs and OG stand for the agricultural site, 5, 12, 20, 60 years-old secondary forest and old growth forest, respectively. Means, standard deviations (sd) and Kruskal-wallis P-values are reported.

	AG	5yrs	12yrs	20yrs	60yrs	OG	
	mean (sd)	mean (sd)	mean (sd)	mean (sd)	mean (sd)	mean (sd)	P-value
Stem density (stem ha ⁻¹)	-	606.3 (39.0) ^a	456.3 (43.8) ^{abc}	564.6 (140.6) ^{ab}	410.4 (74.0) ^{bc}	395.8 (52.0) ^c	0.04
Plot BA (m ² ha ⁻¹)	-	15.9 (6.4) ^a	22.7 (3.4) ^{ab}	23.7 (4.9) ^{ab}	25.7 (1.8) ^{ab}	35.7 (2.9) ^b	0.04
Plot AGB (Mg ha ⁻¹)	-	42.5 (17.4) ^a	79.8 (17) ^{ab}	96 (28.1) ^{ab}	182 (10.4) ^b	427.8 (105.8) ^c	0.012
Clay (%)	6.4 (4.5)	8.8 (7.4)	9.1 (5.1)	8.3 (8.2)	12.8 (10.1)	14.1 (6.4)	0.32
Silt (%)	6.9 (5.5)	7.5 (5.0)	8 (5.9)	9.3 (9.2)	5.9 (6.2)	5.3 (3.3)	0.66
Sand (%)	86.7 (7.5)	83.7 (10.8)	82.9 (6.2)	82.4 (11.4)	81.3 (10.4)	80.5 (6.4)	0.49
BD (g cm ⁻³)	1.3 (0.1) ^{ab}	1.1 (0.2) ^{bc}	1.3 (0.1) ^a	1.2 (0.1) ^{abc}	1.2 (0.1) ^{abc}	1.1 (0.1) ^c	0.034
SOC (%)	0.7 (0.3)	1.1 (0.8)	0.5 (0.3)	0.9 (0.3)	0.8 (0.5)	3.3 (1.0)	0.43
pH H ₂ O top soil (0–10 cm)	-	4.7 (0.1) ^a	4.8 (0.2) ^a	4.7 (0.1) ^{ab}	4.5 (0.1) ^c	4.5 (0.1) ^{bc}	0.002

Nitrogen deposition and leaching: sampling protocol, sample and data analysis

The bulk precipitation, throughfall and lysimeter samples were collected weekly during one hydrological year (i.e. from July 2018 to August 2019) in the three agricultural plots and the twelve secondary forest plots (i.e. 5yrs, 12yrs, 20yrs and 60yrs). The OG plots were not sampled for N deposition and leaching because of logistical constraints but these plots were already studied earlier (see Bauters et al. 2018, 2019). The bulk precipitation and throughfall samples were collected using polyethylene (PE) funnels, supported by a wooden pole of 1.5 m height that was connected to a 5-L PE container with a PE tube. A nylon mesh was placed in the neck of the funnels to avoid contamination of the collected water by large particles. The containers were buried and covered by litter to avoid the growth of algae and to keep the samples cooler. In total, we used a network of 144 collectors (i.e. 120 collectors for 15 plots of throughfall in the forest plots and 24 collectors of 3 plots of bulk precipitation in the agricultural plots). The setup of

bulk and throughfall collectors consisted of a rectangle of 8 by 24 m with 8 m distance between each collector.

Soil solution at 80 cm depth was sampled with 4 lysimeters per plot, installed in the vicinity of the throughfall and bulk precipitation collectors. These 'suction cup' lysimeters consisted of a PVC tube fitted with a porous ceramic cup (Eijkelkamp Soil and Water, Giesbeek, The Netherlands) and connected to a buried opaque 2-L glass bottle by a PE tube. Using a battery-powered vacuum pump (Prenart Equipment, Copenhagen, Denmark), we applied an underpressure of -500 hPa at each sampling occasion.

For the throughfall, open field rainfall, and lysimeter sampling, the weekly sampling protocol was identical. As such, the water volume of each collector was measured in the field and the materials (i.e. recipients, funnels, mesh) were replaced and subsequently rinsed with distilled water. A plot-level composite sample of each collector category was made, considering the volume of each individual sample. These samples were transported to the lab in Kisangani, filtered with a 0.45 μm nylon membrane filter and put in the freezer for storage within 24 hours. Finally, the samples were shipped in batch to Ghent University in Belgium for chemical analysis. The NH_4^+ concentration was determined colorimetrically by the salycilate-nitroprusside method (Mulvaney 1996) on an autoanalyzer (AA3; Bran and Luebbe, Norderstedt, Germany) while NO_3^- was measured by Ion Chromatography (Thermo-Scientific, Pittsburgh, Pennsylvania, USA). Due to some technical problems a bunch of samples was not analyzed for NH_4^+ . Total dissolved nitrogen (TDN) was determined in the water samples with the persulfate oxidation method. For this, an oxidizing solution containing NaOH, H_3BO_3 and $\text{K}_2\text{S}_2\text{O}_8$ was added to the sample (Yasui-tamura et al. 2020), which was subsequently placed in an autoclave at 121°C for 1 hour in order to convert NH_4^+ and dissolved organic N (DON) into NO_3^- . We calculated the DON concentration as the difference between TDN and the sum of NH_4^+ and NO_3^- analyzed in a non-digested sample.

The water flux for bulk precipitation and throughfall was calculated by dividing the average water volume by the surface area of the funnel. We calculated the intercept evaporation at plot scale as the difference between rainfall and throughfall under the assumption that the stem flow was negligible (Zimmermann et al. 2013). Nitrogen deposition fluxes were calculated by multiplying the water volumes with the corresponding concentration of N species. Further, we used the filtering approach of the canopy budget model to estimate dry deposition and canopy exchange from the throughfall and bulk precipitation data (Ulrich 1983; Van Langenhove et al. 2020). Consequently, the total atmospheric deposition was obtained by summing the bulk and the dry deposition, and the canopy exchange by subtracting total atmospheric deposition from throughfall deposition. The N leaching flux at 80 cm depth was calculated by the chloride mass balance (CMB) method (De Schrijver et al. 2004). This method is based on the assumption of mass conservation between the input of atmospheric chloride and the chloride flux in the subsoil (Eriksson and Khunakasem 1969).

Soil N metrics

We sampled topsoil (0–10 cm depth) at five locations and combined them into one composite sample per plot. The samples were oven dried at 60°C for 48h, homogenized and analyzed. The N content and $\delta^{15}\text{N}$ was determined using an elemental analyzer (automated nitrogen carbon analyzer; ANCA-SL, SerCon, UK), interfaced with an isotope ratios mass spectrometer (IRMS; 20–22, SerCon, UK). The soil texture was determined by the pipet method (Burt, 2004). After removal of the organic matter with H_2O_2 30%, soil particles were dispersed by $\text{Na}_4\text{P}_2\text{O}_7$ (aq). The total soil N stock was calculated as the product of soil N content, bulk density, and the soil upper 10 cm, and extrapolated to the plot-scale surface area. We extracted NH_4^+ and NO_3^- with 1M KCl. For each sample, 30g soil was extracted with 60 ml 1M KCl, shaken for 1h and filtered (MN615; Macherey-Nagel, Darmstadt, Germany). The NH_4^+ and NO_3^- concentrations in the KCl extracts were determined colorimetrically using an auto analyzer (AA3; Bran and Luebbe, Norderstedt, Germany).

Nitrous oxide (N_2O) emissions were determined every two weeks during one hydrological year (e.g. from April 2019 to May 2020 because of delayed arrival of static chambers at the study site) using manual static chambers (Hutchinson and Mosier 1981). The chamber bases were installed permanently to avoid soil disturbance. We used chambers made of PVC (diameter = 0.3 m, height = 0.3 m), equipped with an airtight lid, thermocouples, sampling ports, and a vent tube to avoid pressure disturbances. On every sampling occasion, chambers were closed for 1h and the headspace samples taken at 20 minutes interval using a 20 mL syringe and stored in pre-evacuated 12mL containers (Exetainer, Labco, Lampeter, UK). At each sampling time point, temperature inside the chamber was measured using a thermocouple (Type T, Omega Engineering, Stanford, CT, USA). The samples were analyzed at ETH Zurich for N_2O using gas chromatography (456-GC; Scion Instruments, Livingston, UK). We calculated the N_2O fluxes according to Eq. 1.

$$F = [(V \cdot P) / (R \cdot S \cdot T)] \cdot \Delta C / \Delta t \text{ (Eq. 1)}$$

Where V is the volume of static chamber, P is the pressure, R is the gas constant ($0.08206 \text{ [L atm K}^{-1} \text{ mol}^{-1}]$), S is the area, T is the temperature and $\Delta C / \Delta t$ is the slope of linear regression model representing the rate of concentration change in one hour.

Plant N metrics

A tree species inventory was conducted in the 40 by 40 m plots. The diameter at breast height (DBH) of trees with diameter ≥ 10 cm was measured, marked, and identified at species level. Fully expanded, sun leaves were sampled from the canopy for all species that contributed to 85% of the cumulative plot basal area. The leaves were oven-dried at 70°C for 48h and ground before chemical analyses. Leaf C and N content and leaf $\delta^{15}\text{N}$ were analyzed using an elemental analyzer (ANCA-SL, SerCon, UK), interfaced with an isotope ratio mass spectrometer (20–22, SerCon, UK). We further calculated the community-weighted mean (CWM) for these measured leaf functional traits, weighed with basal area per species per plot.

Litter traps (diameter = 0.68 m) were installed in parallel to the throughfall funnels. Consequently, as for throughfall, eight litter traps per plots were set up in a rectangular 8 by 24 m sub-plot and were sampled once a week from July 2018 to August 2019 in twelve plots of secondary forests (5yrs, 12yrs, 20yrs and 60yrs). As we were interested in the fine litterfall, branches of diameter > 2 cm were discarded when present in our traps. Subsequently, litter samples were oven dried at 70°C for 24 hours, weighed and ground before chemical analysis. A subset of litter samples, selected to be representative of seasons, was analyzed for N content using an elemental analyzer (ANCA-SL, SerCon, UK). The litter N flux was calculated by multiplying litter mass by litter N content.

We used ingrowth cores to assess fine roots production from December 2019 to February 2021. The sampling was conducted with 3 month intervals according to an established protocol (Metcalf et al. 2007; Marthews et al. 2014). We washed the fine roots, oven dried them for 24h at 70°C, and finally weighted and ground them before chemical analysis. The amount of root dry mass collected after three months represents the trimestral root production and subsequently the annual production is the sum of the trimestral production. A subset of root samples, selected to be representative of seasons, was analyzed for N content using an elemental analyzer (ANCA-SL, SerCon, UK). The contribution of fine root production to the plot N was calculated by multiplying the fine root mass production by the corresponding fine root N content.

Statistical analysis

We conducted one-way analysis of variance (ANOVA) to test the variation of the different components of the N cycle and metrics among successional stages. Additionally, we applied the Tuckey HSD post-hoc test. In case the underlying assumptions of ANOVA, mainly homoscedasticity and normality, were not met, we used the Kruskal-Wallis and subsequently its post-hoc Dunn's test to analyze the data. We performed the statistical analyses using the R programming language 3.6.1 (R Development core 2018).

Results

Water fluxes

During the one hydrological year of our sampling, the recorded rainfall volume for the study site was of 2134 ± 44.6 mm. None of the analyzed components of the hydrological cycle showed a significant change with forest age. The canopy interception was at lowest in the 20 years-old forests. The relative interception was $15.8 \pm 8.9\%$, $14.8 \pm 6.4\%$, $7.1 \pm 12.1\%$ and $13.4 \pm 5.3\%$ in 5, 12, 20 and 60 years-old secondary forests, respectively (Figure S1). Throughfall was 1700 ± 302 , 1767 ± 241 , 1973 ± 298.8 and 1833 ± 170 mm in the 5, 12, 20 and 60 years-old secondary forest (Figure S1 and Table S2). Leaching at 80 cm depth was 1232 ± 340 mm, 684 ± 238 mm, 973 ± 172 mm, 1157 ± 116 mm and 964 ± 433 mm in the AG and 5, 12, 20 and 60 years-old secondary forests, respectively (Figure S1).

Nitrogen input and output fluxes

The overall amount of N that reached the forest floor via throughfall was affected by the forest stand age via the canopy complexity and composition (Figure 2, Table S1). During the first twenty years of succession the forests show negative values of canopy exchange that is indicative of net canopy N uptake and conservation (Table S1). The net canopy N uptake varied between 2.5% and 44.1% of total atmospheric N deposition. Secondly, young secondary forests (up to 20 years) showed a reduced canopy efficiency and high plot to plot variation in trapping dry N particles (Table S1). The 60 years secondary forests showed a high efficiency for trapping atmospheric dry N particles and positive canopy exchange values indicative of net canopy leaching (Table S1). Consequently, the amount of N reaching the forest floor (throughfall) was significantly higher in the 60 years secondary forests ($P = 0.044$, $P = 0.026$, $P = 0.005$, $P = 0.004$ for ammonium, nitrate, DON and TDN, respectively). Wet and dry deposition contributed proportionally to the throughfall deposition in the 60 years old forest (being respectively 39% and 36%) and the canopy leaching contributed 25%.

In general, we observed a decrease in the leaching fluxes from AG to the 20 years-old secondary forest (Figure 2, Table S1) and a re-increase above 20 years of succession. In the 60 years secondary forests, the leached NO_3^- showed variable $\delta^{15}\text{N}$ and a low $\delta^{18}\text{O}$ signature, while $\delta^{18}\text{O}$ was higher for the other successional stages (Figure S3). The partial atmospheric deposition – leaching balance was negative in the AG sites and approached zero after the first decade of succession (Figure 2). Moreover, N concentration in the leachate of the agricultural sites showed a consistent decreasing trend over the time and were considerably higher during the first half of the sampling period (Figure S2). Additionally, N_2O fluxes increased significantly along the successional stages ($P = 0.0062$). The agricultural field and 60 years-old forest showed the lowest and highest values, respectively (Figure 3). The total soil N and the available N pool (NH_4^+ and NO_3^-) and soil $\delta^{15}\text{N}$ did not show a consistent change with forest succession status (Figure S4).

Tissue N

The weighted foliar N and C:N ratio increased and decreased, respectively, along the successional gradient and thus showed higher and lower values in the late successional stages (Figure 3, Table S4). Weighted foliar $\delta^{15}\text{N}$ and foliar N content were maximal in the late successional stages (i.e., 60 years-old secondary forest and old growth forest), though the foliar $\delta^{15}\text{N}$ also showed a decreasing trend early on the succession (Figure 3). Overall, the N recycled internally through leaf litter and fine root fluxes did not significantly change with successional stage. However, the amount of N transferred by litter deposition increased with stand age and ranged between $119 \pm 45 \text{ kg N ha}^{-1} \text{ yr}^{-1}$ and $178 \pm 51 \text{ kg N ha}^{-1} \text{ yr}^{-1}$ (Figure 3). The litter N concentration showed an increasing trend over time with the highest value in the late successional stages. The litter C:N ratios were low in the 60 years-old growth forests. The N amount assimilated by the fine roots was ranged between $47 \pm 5 \text{ kg N ha}^{-1} \text{ yr}^{-1}$ and $139 \pm 47 \text{ kg N ha}^{-1} \text{ yr}^{-1}$ (Figure 3). Fine root N concentration (%) and fine root C:N ratio showed higher and lower values in the late successional stages, respectively.

Discussion

Hydrologic balance

Structural vegetation parameters, such as basal area and canopy height, consistently changed along the successional gradient at our study site (Makelele et al., 2021). But an effect of forest structure recovery on water fluxes was only observed in the first decade of succession. Interception was highest in the 5 years-old forests, while leaching was maximal in the agricultural sites and minimal in the 5 and 12 years-old forests (Figure S1). The relative interception values are between the range of values found previously at our study site (i.e. 6% and 17%, Bauters et al. 2019), but are relatively low compared to the global forest interception average (Magliano et al. 2019; Yue et al. 2021). Forest composition and structure or individual species' crown morphology plays an important role in water interception (Yang et al. 2019; Yue et al. 2021). As such, high interception earlier in the succession could be attributable to the crown shape of *Musanga cecropioides*, the umbrella tree, dominating young secondary forest of the Congo basin and closing the canopy within the first years of forest regrowth (Ross 1954). On the other hand, Zimmermann et al. (2013) attributed recovery of forest interception to vegetation structure restoration in the Brazilian Amazon. However, contrasting results have been found in Mexican mountain forests where interception after 20 years forest regrowth was 50% of that of mature forest due to slow recovery of leaf area index and epiphytic biomass (Muñoz-Villers et al. 2012). High leaching from the agricultural site is the result of reduced vegetation interception and evaporation (Bruijnzeel 2004; Zimmermann et al. 2013). The reduced leaching in the 5-year-old forest may result from increased interception and legacy of soil impermeability from the previous agriculture activities (Bruijnzeel 2004). Globally, the effect of forest disturbance on the hydrological cycle depends on site, hydro-climate and landscape characteristics (Sandström 1995). Here, we show that the effect of shifting cultivation on the forest ecosystem hydrological process is only observed during the first years of succession (see also, Zimmermann et al. 2013).

Bulk and throughfall N deposition

One of the major environmental consequences of N pollution on the planet is the increase in atmospheric N deposition (Stevens 2019). Recent research has shown that the Congo basin is a hotspot for N deposition (Bauters et al. 2018, 2019), even more than previously predicted (Reay et al. 2008). Here, we confirm that the Congo basin is subjected to a high bulk N deposition (i.e. open field deposition) of $11.6 \pm 2.6 \text{ kg N ha}^{-1} \text{ yr}^{-1}$, lower but comparable to $18.2 \text{ kg N ha}^{-1} \text{ yr}^{-1}$ that has been previously found (Bauters et al. 2018). We also corroborated that DON is contributing roughly 50% to TDN deposition. The amount of bulk N deposition for the central Congo basin is substantially higher than what has been found previously in Central and South America, Southeast Asia and West Africa (Williams et al. 1997; Oziegbe et al. 2011; Kohler et al. 2013; Van Langenhove et al. 2020). For example, for a study using the same field protocol as this study conducted in French Guiana, the amount of TDN and inorganic N (NH_4^+ and NO_3^-) was, respectively, two and four times lower than what we found (Van Langenhove et al. 2020). However, the relative proportion of DON measured in French Guiana was in the same range, indicating that omitting DON quantification underestimates the magnitude of N deposition in tropical forests. In contrast to

industrial and emerging countries, where elevated N deposition is derived from industrial and intensive agriculture activities, elevated N deposition at our study site is sourced from biomass burning (Chen et al. 2010; Bauters et al. 2019). Chen et al. (2010) estimated that between 50 and 80% of the N deposited in the Congo basin, South American and Southeast Asian tropical forest is fire-derived. Indeed, Bauters et al. (2018) showed that TDN deposited on forests of the Congo basin was linked to the biomass burning intensities in the prevailing wind directions over the seasons. Further, they showed a positive correlation between DON deposition and the concentration of condensed aromatics in rainfall, which are organic compounds that are exclusively sourced by combustion.

Furthermore, in this study, we show how the canopy composition and complexity, through dry particle interception and canopy exchange, sensibly modify the amount of N that reaches the forest floor by means of throughfall. Vegetation structure attributes, such as canopy height and density, play a great role in trapping atmospheric particles (Lawrence et al. 2008; Runyan et al. 2013; Powers and Marín-Spiotta 2017). Indeed, more complex canopies have been shown more efficient in trapping atmospheric particles and nutrients (Runyan et al. 2013; Bauters et al. 2021a) such that the amount of nutrients deposited increases with the canopy complexity along secondary succession (Bauters et al. 2021a). Consequently, the change of forest composition and structure as the succession proceed (Bauters et al. 2021a; Makelele et al. 2021) results in increasing total N deposition as shown here (i.e. between 12 and 60 years-old forests). The amount of N deposited locally can be highly variable and in some cases dependent on the distance between the site and an active slash-and-burn field and on the landscape configuration (Kohler et al. 2013). Kohler et al (2013) showed that plots closed to an active slash-and-burn field receive more atmospheric N as N-NO_3^- in comparison to plots located deep in the forest and relatively far from slash-and-burn activities. The distance between each individual plot and an active slash-and-burn field (Figure 1) is potentially responsible for the high variability of atmospheric N deposition in young secondary forest (Table S1) and the unexpected high N deposition in the 5 years secondary forest. On the other hand, our results suggest that young secondary forest substantially rely on canopy N uptake, likely to compensate N limitation. Indeed, the canopy may also retain a substantial amount of N via leaves stomata and cuticle absorption (Bortolazzi et al. 2021). In contrast, canopy N leaching in the 60 years secondary forest may be indicative of N saturation of aged tropical forests. Altogether, the forests of the Congo basin are receiving high amounts of N from biomass burning occurring in shifting cultivation systems in the forest and savannah biomes of the Congo basin. However, the forest's successional status affects the amount of N that reaches the forest floor, through canopy trapping and exchange. On this basis, we postulate that the main external sources of N for tropical forest of the Congo basin shift from BNF in the youngest forests (Bauters et al. 2016) to atmospheric N deposition in the older forests. As such the canopy composition and complexity play an important role in the recuperation of the N cycle after a shifting cultivation event.

Soil and leaching N fluxes

The available and total soil N stocks (Fig. S4) did not change with the forest successional status. This finding corroborates with a number of studies from the Neotropics and South East Asia (e.g. Markewitz et

al. 2004; Winbourne et al. 2018; Kukla et al. 2019). Relatively extensive agricultural activity such as the shifting cultivation at our study site tends to preserve nitrogen (Bauters et al. 2021b). The conservation of substantial N in the soil should facilitate rapid recuperation of many processes of the N cycle (Davidson et al. 2007; Winbourne et al. 2018). However, the projected population growth in the Democratic Republic of Congo will likely result in a more intense (i.e. reduction in lengths of fallow cycle) shifting cultivation. The reduction of fallow periods and the repeated slash-and-burn cycles deplete soil N and other nutrients and might ultimately affect the recuperation trajectory of N and vegetation in the traditional shifting cultivation systems (Moonen *et al.*, 2019; Bauters *et al.*, 2021).

The N leaching fluxes were strikingly high in the agricultural sites and mostly composed of NO_3^- . The leached NO_3^- showed elevated $\delta^{18}\text{O}$ values for all the successional stages, except the 60 years-old secondary forests (Figure S3), implying that the leached NO_3^- is at least partly composed of NO_3^- directly derived from atmospheric deposition. The effect of fire on N leaching in a shifting cultivation system is sensibly detectable in the six first months (Figure S2) that follow field burning (see also, da Silva Neto *et al.*, 2019 for the effect on soil properties). The high N leaching flux during the agricultural phase is thus most likely a combined result of: (1) enhanced soil water recharge (Figure S1, see also Owuor et al. 2016); (2) preceding burning, which increases soil available nutrients by incorporating nutrient rich-ash from aboveground biomass burning in the soil along with the chemical alteration of soil organic matter and biomass (Murphy et al. 2006; Kukla et al. 2019), and (3) reduced vegetation N uptake, especially before crop planting. Further, we showed that the amount of N ($24.5 \pm 29 \text{ kg N ha}^{-1} \text{ yr}^{-1}$) leached from the 60-years-old was higher compared to the findings of Bauters *et al.* (2019) in mature mixed and monodominant lowland forests at our study site, where they reported soil-leaching fluxes of 11.5 ± 2.8 and $15.0 \pm 5.5 \text{ kg N ha}^{-1} \text{ yr}^{-1}$, respectively.

N cycle recuperation

A recuperation of the N cycle during secondary succession is reflected in most analyzed plant tissue-based N metrics. We showed an increasing tissue N content and decreasing tissue C:N ratios along the succession. The latter is consistent with increasing N availability (Davidson et al. 2007; Hietz et al. 2011). Foliar $\delta^{15}\text{N}$ values of the central Congo basin ($3.1\text{‰} \pm 0.8\text{‰}$ to $6.8\text{‰} \pm 0.3\text{‰}$) fall within the range of values for the Amazon forest (0.9‰ to 10.0‰ , Ometto et al. 2006; Davidson et al. 2007). The canopy $\delta^{15}\text{N}$ signal translates ecosystem N processes and N input-output budgets (Compton et al. 2007). Conceptually, increasing N availability during secondary succession due to BNF and atmospheric N deposition results in loss of $\delta^{15}\text{N}$ depleted N species and thus $\delta^{15}\text{N}$ enrichment (Amundson et al. 2003). Our foliar $\delta^{15}\text{N}$ data show two trends in the recuperation process of the N cycle of the central Congo basin: (1) initial higher foliar $\delta^{15}\text{N}$ as a result from biomass burning is reduced during the first 20 years of succession due to ^{15}N depletion resulting from BNF – a trend corroborated by several earlier studies (Compton et al. 2007; Wang et al. 2007; Broadbent et al. 2014), and (2) after 20 years into the succession, we show a re-increase of foliar $\delta^{15}\text{N}$ likely due to a declining BNF (Bauters et al. 2016) gradual increasing N availability, leading to increasing gaseous (Figure 4) and hydrological loss in the late successional

stage, which enriches the remaining plant available N pool in ^{15}N (Amundson et al. 2003; Davidson et al. 2007).

In line with this trend in foliar $\delta^{15}\text{N}$, we showed a decreasing N leaching in the young forest and a re-increase during the late successional stages (Figure 4). In contrast to the findings of Bauters et al. (2019) in a mature mixed forest, we showed that mineral N (mostly NO_3^-) was the dominant leaching N species, which is in accordance to a more open N cycle in the late successional stages of tropical forests (Hedin et al. 2009; Elser 2011; Brookshire et al. 2012). In addition, we showed that all the deposited N in the late successional stage is fully recycled in the system before leaching, while the leaching N in the younger forests are composed of a mix between the atmospheric deposition and soil N (Figure S3).

The transition of a more conservative N cycle in the young secondary tropical forest to a more open N cycle in late successional tropical forest is associated with increasing N_2O emissions (Davidson et al. 2007). We showed increasing soil emissions of N_2O along the successional stages. These trends corroborate with findings from similar studies from the Neotropics (Davidson et al. 2007) and South East Asia (Wang et al. 2021) with N_2O emissions increasing from 3 to 70 years and 12 to 54 years of succession, respectively. Low N_2O emissions in a young secondary forest results from high N losses during the agricultural phase and is thus generally used as an indicator of a conservative N cycle of younger forests. The N_2O emissions in the 60 years-old secondary forest was double the amount emitted in the lowland OG forests (Figure 4, see also Gallarotti et al. 2021; Barthel et al. 2022) and above the global tropical forest N_2O emissions mean (Werner et al. 2007), but it was similar to the emissions in a secondary forest in Cameroun (Verchot et al. 2020) and OG forests in Ghana (Castaldi et al. 2013) and Congo (Serca et al. 1994). The N_2O emission peak in the 60 years-old secondary forest additionally indicates that the N cycle is recovering to its status in a mature forest, following shifting cultivation (Winbourne et al. 2018).

Overall, a recuperation of a typically open N cycle of a mature lowland tropical forest is, in many cases, associated with increasing N_2O emissions, increasing foliar $\delta^{15}\text{N}$ as well as foliar, litter and root N content and decreasing foliar, root and litter C:N ratios, in line with what earlier studies reported (Davidson et al. 2007; Sullivan et al. 2019). In conclusion, and in accordance with the points developed above, our data depict such a recuperation process despite elevated atmospheric N deposition. As such, this also suggests that N deposition does not alleviate N limitation early-on in secondary successions in Central Africa.

Declarations

Acknowledgements

The Belgian Development Cooperation has supported this research by funding the VLIR-UOS team project, forest ecosystem monitoring in the Congo (FORMONCO II). VLIR-UOS supports partnerships

between universities and university colleges in Flanders (Belgium) and universities in Africa, Latin America and Southeast Asia, looking for innovative responses to global and local challenges. FORMONCO II was a collaboration between researchers from Ghent University, Université de Lubumbashi, Université de Kisangani, Université Catholique de Bukavu. We specially thank the Professor Oswald Van Cleemput for accepting to conduct the 'internal review' of our manuscript.

Funding

The Belgian Development Cooperation has supported this research by funding the VLIR-UOS team project, forest ecosystem monitoring in the Congo (FORMONCO II)

Competing Interests

Author declare no competing interests

Author contributions

MAI, MB, KV and PB designed the experiment; MAI and MB conducted the experiment and analyzed the samples; MAI and MB conducted the statistical analyses; MAI, with contributions from MB, PB and KV, wrote the paper; all co-authors discussed the results and commented on the manuscript.

References

1. Amundson R, Austin AT, Schuur EAG, et al (2003) Global patterns of the isotopic composition of soil and plant nitrogen. *Global Biogeochem Cycles* 17:1031–1041. <https://doi.org/10.1029/2002GB001903>
2. Barron AR, Purves DW, Hedin LO (2011) Facultative nitrogen fixation by canopy legumes in a lowland tropical forest. *Oecologia* 165:511–520. <https://doi.org/10.1007/s00442-010-1838-3>
3. Barthel M, Bauters M, Baumgartner S, et al (2022) Low N₂O and variable CH₄ fluxes from tropical forest soils of the Congo Basin. *Nat Commun* 13:1–8. <https://doi.org/10.1038/s41467-022-27978-6>
4. Batterman SA, Hedin LO, Breugel M Van, et al (2013) Key role of symbiotic dinitrogen fixation in tropical forest secondary succession. *Nature* 502:224–227. <https://doi.org/10.1038/nature12525>
5. Baumgartner S, Barthel M, Drake T, et al (2020) Seasonality, drivers, and isotopic composition of soil CO₂ fluxes from tropical forests of the Congo Basin. *Biogeosciences* 17:6207–6218. <https://doi.org/10.5194/bg-2020-133>
6. Bauters M, Drake TW, Verbeeck H, et al (2018) High fire-derived nitrogen deposition on central African forests. *Proc Natl Acad Sci U S A* 115:549–554. <https://doi.org/10.1073/pnas.1714597115>
7. Bauters M, Drake TW, Wagner S, et al (2021a) Fire-derived phosphorus fertilization of African tropical forests. *Nat Commun* 12:5129. <https://doi.org/10.1038/s41467-021-25428-3>
8. Bauters M, Mapenzi N, Kearsley E, et al (2016) Facultative nitrogen fixation by legumes in the central Congo basin is downregulated during late successional stages. *Biotropica* 48:281–284.

<https://doi.org/10.1111/btp.12312>

9. Bauters M, Moonen P, Summerauer L, et al (2021b) Soil Nutrient Depletion and Tree Functional Composition Shift Following Repeated Clearing in Secondary Forests of the Congo Basin. *Ecosystems* 24:1422–1435. <https://doi.org/10.1007/s10021-020-00593-6>
10. Bauters M, Verbeeck H, Rütting T, et al (2019) Contrasting nitrogen fluxes in African tropical forests of the Congo Basin. *Ecol Monogr* 89:e01342. <https://doi.org/10.1002/ecm.1342>
11. Bortolazzi A, Da L, Rodeghiero M, et al (2021) The canopy layer , a biogeochemical actor in the forest N-cycle. *Sci Total Environ* 776:146024. <https://doi.org/10.1016/j.scitotenv.2021.146024>
12. Broadbent EN, Zambrano MA, Asner GP, et al (2014) Integrating Stand and Soil Properties to Understand Foliar Nutrient Dynamics during Forest Succession Following Slash-and-Burn Agriculture in the Bolivian Amazon. *PLoS One* 9:e86042. <https://doi.org/10.1371/journal.pone.0086042>
13. Brookshire ENJ, Hedin LO, Newbold JD, et al (2012) Sustained losses of bioavailable nitrogen from montane tropical forests. *Nat Geosci* 5:123–126. <https://doi.org/10.1038/ngeo1372>
14. Bruijnzeel LA (2004) Hydrological functions of tropical forests: Not seeing the soil for the trees? *Agric Ecosyst Environ* 104:185–228. <https://doi.org/10.1016/j.agee.2004.01.015>
15. Castaldi S, Bertolini T, Chiti T, Valentini R (2013) Nitrous oxide emissions from soil of an African rain Dynamics forest in Ghana. *Biogeosciences* 10:4179–4187. <https://doi.org/10.5194/bg-10-4179-2013>
16. Chen Y, Randerson JT, Werf GR VAN DER, et al (2010) Nitrogen deposition in tropical forests from savanna and deforestation fires. *Glob Chang Biol* 16:2024–2038. <https://doi.org/10.1111/j.1365-2486.2009.02156.x>
17. Compton JE, Hooker TD, Perakis SS (2007) Ecosystem N Distribution and d N during a Century of Forest Regrowth after Agricultural Abandonment. *Ecosystems* 10:1197–1208. <https://doi.org/10.1007/s10021-007-9087-y>
18. Curtis PG, Slay CM, Harris NL, et al (2018) Classifying drivers of global forest loss. *Science* (80-) 361:1108–1111. <https://doi.org/10.1126/science.aau3445>
19. da Silva Neto EC, Pereira MG, Carvalho E, et al (2019) Temporal evaluation of soil chemical attributes after slash-and-burn agriculture in the Western Brazilian Amazon. *Acta Sci* 41:1–10. <https://doi.org/10.4025/actasciagron.v41i1.42609>
20. Davidson EA, Davidson EA, Ishida Y, et al (2007) Recuperation of nitrogen cycling in Amazonian forests following agricultural abandonment. *Nature* 447:995–998. <https://doi.org/10.1038/nature05900>
21. Davidson EA, Martinelli LA (2009) Nutrient Limitations to Secondary Forest Regrowth. In: Michael Keller, Mercedes Bustamante, John Gash PSD (ed) *Amazonia and Global Change*. AGU, Washington, DC, pp 299–309
22. De Ridder M, Toirambe B, Bulcke J Van Den, et al (2014) Dendrochronological Potential in a Semi-Deciduous Rainforest: The Case of. *Forests* 5:3087–3106. <https://doi.org/10.3390/f5123087>

23. De Schrijver A, Nachtergale L, Staelens J, et al (2004) Comparison of throughfall and soil solution chemistry between a high-density Corsican pine stand and a naturally regenerated silver birch stand. *Environ Pollut* 131:93–105. <https://doi.org/10.1016/j.envpol.2004.01.019>
24. de Wasseige C, de Marcken P, Bayol N, et al (2012) *Les forêts du bassin du Congo: État des Forêts 2010*. Office des publications de l'Union, Luxembourg
25. Du E, Terrer C, Pellegrini AFA, et al (2020) Global patterns of terrestrial nitrogen and phosphorus limitation. *Nat Geosci* 13:221–226. <https://doi.org/10.1038/s41561-019-0530-4>
26. Elser JJ (2011) A world awash with Nitrogen. *Science* 334:1504–1505. <https://doi.org/10.1126/science.1215567>
27. Eriksson E, Khunakasem V (1969) Chloride concentration in groundwater, recharge rate and rate of deposition of chloride in the israel coastal plain. *J Hydrol* 7:178–197. [https://doi.org/10.1016/0022-1694\(69\)90055-9](https://doi.org/10.1016/0022-1694(69)90055-9)
28. Figueiredo V, Enrich-Prast A, Rütting T (2019) Evolution of nitrogen cycling in regrowing Amazonian rainforest. *Sci Rep* 9:1–8. <https://doi.org/10.1038/s41598-019-43963-4>
29. Gallarotti N, Barthel M, Verhoeven E, et al (2021) In-depth analysis of N₂O fluxes in tropical forest soils of the Congo Basin combining isotope and functional gene analysis. *ISME J* 15:3357–3374. <https://doi.org/10.1038/s41396-021-01004-x>
30. Gerland P, Raftery AE, Ševčíková H, et al (2014) World Population Stabilization Unlikely This Century. *Science* (80-) 346:234–237. <https://doi.org/10.1126/science.1257469>.World
31. Hedin LO, Brookshire ENJ, Menge DNL, Barron a R (2009) The Nitrogen Paradox in Tropical Forest Ecosystems. *Annu Rev Ecol Evol Syst* 40:613–635. <https://doi.org/10.1146/Annurev.Ecolsys.37.091305.110246>
32. Hietz P, Turner BL, Wanek W, et al (2011) Long-Term Change in the Nitrogen Cycle of Tropical Forests. *Science* (80-) 334:664–666. <https://doi.org/10.1126/science.1211979>
33. Hubau W, Lewis SL, Phillips OL, et al (2020) Asynchronous carbon sink saturation in African and Amazonian tropical forests. *Nature* 579:80–87. <https://doi.org/10.1038/s41586-020-2035-0>
34. Hutchinson GL, Mosier AR (1981) Improved Soil Cover Method for Field Measurement of Nitrous Oxide Fluxes. *Soil Sci Soc Am J* 45:311–316. <https://doi.org/10.2136/sssaj1981.03615995004500020017x>
35. Jenny H (1950) Causes of the high nitrogen and organic matter content of certain tropical forest soils. *Soil Sci* 69:63–69. <https://doi.org/10.1097/00010694-195001000-00005>
36. Kohler S, Jungkunst HF, Eramsi S, Gerold G (2013) The effects of land use change on atmospheric nutrient deposition in central Sulawest. *Erdkunde* 2:109–122. <https://doi.org/10.3112/erdkunde.2013.02.01>
37. Kukla J, Whitfeld T, Petr C, et al (2019) The effect of traditional slash - and - burn agriculture on soil organic matter , nutrient content , and microbiota in tropical ecosystems of Papua New Guinea. *L Degrad Dev* 30:166–177. <https://doi.org/10.1002/ldr.3203>

38. Lawrence D, Odorico PD, Delonge M, et al (2008) Ecological feedbacks following deforestation create the potential for a catastrophic ecosystem shift in tropical dry forest. PNAS 104:20696–20701. <https://doi.org/10.1073/pnas.0705005104>
39. Magliano PN, Whitworth-Hulse JI, Baldi G (2019) Interception, throughfall and stemflow partition in drylands: Global synthesis and meta-analysis. J Hydrol 568:638–645. <https://doi.org/10.1016/j.jhydrol.2018.10.042>
40. Makelele IA, Verheyen K, Boeckx P, et al (2021) Afrotropical secondary forests exhibit fast diversity and functional recovery, but slow compositional and carbon recovery after shifting cultivation. J Veg Sci 32:e13071. <https://doi.org/10.1111/jvs.13071>
41. Markewitz D, Davidson E, Moutinho P, Nepstad D (2004) Nutrient loss and redistribution after forest clearing on highly weathered soil in amazonia. Ecol Appl 14:177–199. <https://doi.org/10.1890/01-6016>
42. Marthews TR, Riutta T, Menor IO, et al (2014) Measuring Tropical Forest Carbon Allocation and Cycling (v3.0). Manual, Global Ecosystems Monitoring network. <http://gem.tropicalforests.ox.ac.uk/>
43. Martin PA, Newton AC, Bullock JM (2013) Carbon pools recover more quickly than plant biodiversity in tropical secondary forests. Proc R Soc B Biol Sci 280:20132236. <https://doi.org/10.1098/rspb.2013.2236>
44. Mcgrath DA, Smith CK, Gholz HL, Oliveira FDA (2001) Effects of land-Use change on soil nutrient dynamics in Amazonia. Ecosystems 4:625–645. <https://doi.org/10.1007/s10021-001-0033-0>
45. Metcalfe DB, Williams M, Aragão LEOC, et al (2007) A method for extracting plant roots from soil which facilitates rapid sample processing without compromising measurement accuracy. New Phytol 697–703. <https://doi.org/10.1111/j.1469-8137.2007.02032.x>
46. Meyerholt J, Sickel K, Zaehle S (2020) Ensemble projections elucidate effects of uncertainty in terrestrial nitrogen limitation on future carbon uptake. Glob Chang Biol 26:3978–3996. <https://doi.org/10.1111/gcb.15114>
47. Moonen PCJ, Verbist B, Boyemba Bosela F, et al (2019) Disentangling how management affects biomass stock and productivity of tropical secondary forests fallows. Sci Total Environ 659:101–114. <https://doi.org/10.1016/j.scitotenv.2018.12.138>
48. Muñoz-Villers LE, Holwerda F, Gómez-Cárdenas M, et al (2012) Water balances of old-growth and regenerating montane cloud forests in central Veracruz, Mexico. J Hydrol 462–463:53–66. <https://doi.org/10.1016/j.jhydrol.2011.01.062>
49. Murphy JD, Johnson DW, Miller WW, et al (2006) Wildfire Effects on Soil Nutrients and Leaching in a Tahoe Basin Watershed. J Environ Qual 35:479–489. <https://doi.org/10.2134/jeq2005.0144>
50. Ometto JPHB, Ehleringer JR, Domingues TF, et al (2006) The stable carbon and nitrogen isotopic composition of vegetation in tropical forests of the Amazon Basin , Brazil. Biogeochemistry 79:251–274. <https://doi.org/10.1007/s10533-006-9008-8>
51. Owuor SO, Guzha AC, Rufino MC, et al (2016) Groundwater recharge rates and surface runoff response to land use and land cover changes in semi-arid environments. Ecol Process.

<https://doi.org/10.1186/s13717-016-0060-6>

52. Oziegbe MB, Muoghalu JI, Oke SO (2011) Litterfall , precipitation and nutrient fluxes in a secondary lowland rain forest in Ile – Ife , Nigeria. *Acta Bot Bras* 25:664–671
53. Poorter L, Bongers F, Aide TM, et al (2016) Biomass resilience of Neotropical secondary forests. *Nature* 530:. <https://doi.org/10.1038/nature16512>
54. Porder S, Asner GP, Vitousek PM (2005) Ground-based and remotely sensed nutrient availability across a tropical landscape. *Proc Natl Acad Sci U S A* 102:10909–10912. <https://doi.org/10.1073/pnas.0504929102>
55. Powers JS, Marín-Spiotta E (2017) Ecosystem Processes and Biogeochemical Cycles in Secondary Tropical Forest Succession. *Annu Rev Ecol Evol Syst* 48:497–519. <https://doi.org/10.1146/annurev-ecolsys-110316-022944>
56. Reay DS, Dentener F, Smith P, et al (2008) Global nitrogen deposition and carbon sinks. *Nat Geosci* 1:430–437. <https://doi.org/10.1038/ngeo230>
57. Ross R (1954) Ecological Studies on the Rain Forest of Southern Nigeria: III. Secondary Succession in the Shasha Forest Reserve. *J Ecol* 42:259–282. <https://doi.org/10.2307/2256861>
58. Runyan CW, Odorico PD, Vandecar KL, et al (2013) Positive feedbacks between phosphorus deposition and forest canopy trapping , evidence from Southern Mexico. *Biogeosciences* 118:1521–1531. <https://doi.org/10.1002/2013JG002384>
59. Sandström K (1995) Differences in Groundwater Response to Deforestation - A Continuum of Interactions between Hydroclimate , Landscape Characteristics and Time. *GeoJournal* 35:539–546. <https://doi.org/10.1007/BF00824371>
60. Schmidt SK, Costello EK, Nemergut DR, et al (2007) Biogeochemical Consequences of Rapid Microbial Turnover. *Ecology* 88:1379–1385. <https://doi.org/10.1890/06-0164>
61. Serca D, Delmas R, Jambert C, Labroue L (1994) Tellus B: Chemical and Physical Meteorology Emissions of nitrogen oxides from equatorial rain forest in central Africa : *Tellus* 46B:243–254. <https://doi.org/10.3402/tellusb.v46i4.15795>
62. Slik JWF, Arroyo-Rodríguez V, Aiba SS-I, et al (2015) An estimate of the number of tropical tree species. *Proc Natl Acad Sci* 112:7472–7477. <https://doi.org/10.1073/pnas.1512611112>
63. Stevens CJ (2019) Nitrogen in the environment. *Science* (80-) 363:578–580. <https://doi.org/10.1126/science.aav8215>
64. Suarez RD, Rozendaal DMAA, De Sy V, et al (2019) Estimating aboveground net biomass change for tropical and subtropical forests: refinement of IPCC default rates using forest plot data. *Glob Chang Biol* 25:3609–3624. <https://doi.org/10.1111/gcb.14767>
65. Sullivan BW, Nifong RL, Nasto MK, et al (2019) Biogeochemical recuperation of lowland tropical forest during succession. *Ecology* 100:1-14 e02641. <https://doi.org/10.1002/ecy.2641>
66. Townsend AR, Cleveland CC, Houlton BZ, et al (2011) Multi-element regulation of the tropical forest carbon cycle In a nutshell: *Front Ecol Environ* 9:9–17. <https://doi.org/10.1890/100047>

67. Tyukavina A, Hansen MC, Potapov P, et al (2018) Congo Basin forest loss dominated by increasing smallholder clearing. *Sci Adv* 4:eaat2993. <https://doi.org/10.1126/sciadv.aat2993>
68. Ulrich B (1983) Interaction of forest canopies with atmospheric constituents: So₂, alkali and earth alkali cations and chloride. In: Ulrich B, Pankrath J (eds) *Effects of accumulation of air pollutants in forest ecosystems: proceedings of a workshop held at Goettingen, West Germany, May 16–18, 1982*. Springer, Dordrecht, pp 33–45
69. Van Langenhove L, Verryckt LT, Bréchet L, et al (2020) Atmospheric deposition of elements and its relevance for nutrient budgets of tropical forests. *Biogeochemistry* 149:175–193. <https://doi.org/10.1007/s10533-020-00673-8>
70. Verchot L V, Dannenmann M, Kengdo SK, et al (2020) Land-use change and Biogeochemical controls of soil CO₂, N₂O and CH₄ fluxes in Cameroonian forest landscapes. *J Integr Environ Sci* 17:45–67. <https://doi.org/10.1080/1943815X.2020.1779092>
71. Vitousek PM, Sanford RL, Vitousek PM, Sanford RL (1986) Nutrient cycling in moist tropical forest. *Annu Rev Ecol Syst* Vol 17 137–167. <https://doi.org/10.1146/annurev.es.17.110186.001033>
72. Wang L, Shaner PL, Macko S (2007) Foliar δ¹⁵N patterns along successional gradients at plant community and species levels. *Geophys Res Lett* 34:1–6. <https://doi.org/10.1029/2007GL030722>
73. Wang S, Zuo Q, Cao Q, et al (2021) Acceleration of soil N₂O flux and nitrogen transformation during tropical secondary forest succession after slash-and-burn agriculture. *Soil Tillage Res* 208:104868. <https://doi.org/10.1016/j.still.2020.104868>
74. Werner C, Haas E, Hickler T, Kiese R (2007) A global inventory of N₂O emissions from tropical rainforest soils using a detailed biogeochemical model. *Global Biogeochem Cycles* 21:GB3010. <https://doi.org/10.1029/2006GB002909>
75. Williams MR, Fisher TR, Melack JM (1997) Chemical composition and deposition of rain in the central Amazon, Brazil. *Atmos Environ* 31:207–217. [https://doi.org/10.1016/1352-2310\(96\)00166-5](https://doi.org/10.1016/1352-2310(96)00166-5)
76. Winbourne JB, Feng A, Reynolds L, et al (2018) Nitrogen cycling during secondary succession in Atlantic Forest of Bahia, Brazil. *Sci Rep* 8:1377. <https://doi.org/10.1038/s41598-018-19403-0>
77. Yang B, Kun D, Han L, et al (2019) The effects of tree characteristics on rainfall interception in urban areas. *Landsc Ecol Eng* 15:289–296. <https://doi.org/10.1007/s11355-019-00383-w>
78. Yasui-tamura S, Hashihama F, Ogawa H, Nishimura T (2020) Automated simultaneous determination of total dissolved nitrogen and phosphorus in seawater by persulfate oxidation method. *Talanta Open* 2:100016. <https://doi.org/10.1016/j.talo.2020.100016>
79. Yue K, De Frenne P, Fornara DA, et al (2021) Global patterns and drivers of rainfall partitioning by trees and shrubs. *Glob Chang Biol* 27:3350–3357. <https://doi.org/10.1111/gcb.15644>
80. Zimmermann B, Zimmermann A, Scheckenbach HL, et al (2013) Changes in rainfall interception along a secondary forest succession gradient in lowland Panama. *Hydrol Earth Syst Sci* 17:4659–4670. <https://doi.org/10.5194/hess-17-4659-2013>

Figures

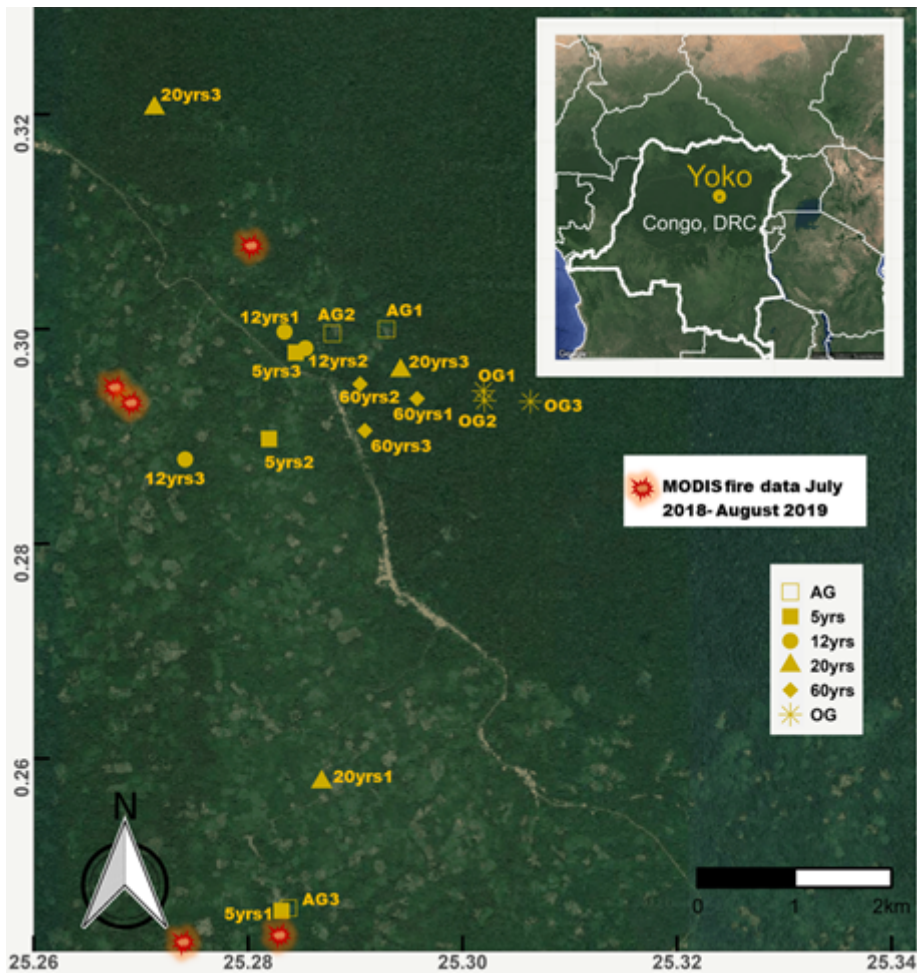


Figure 1

Location of the study area in the Democratic Republic of Congo. The study was conducted in and around the Yoko Forest Reserve (dark yellow circle in the inset) in the central Congo basin. AG, 5yrs, 12yrs, 20yrs, 60yrs and OG indicate the agricultural sites and 5, 12, 20, 60 years-old secondary forests and old growth forest plots, respectively. In addition, slash-and-burn events around our plots during the sampling period are shown.

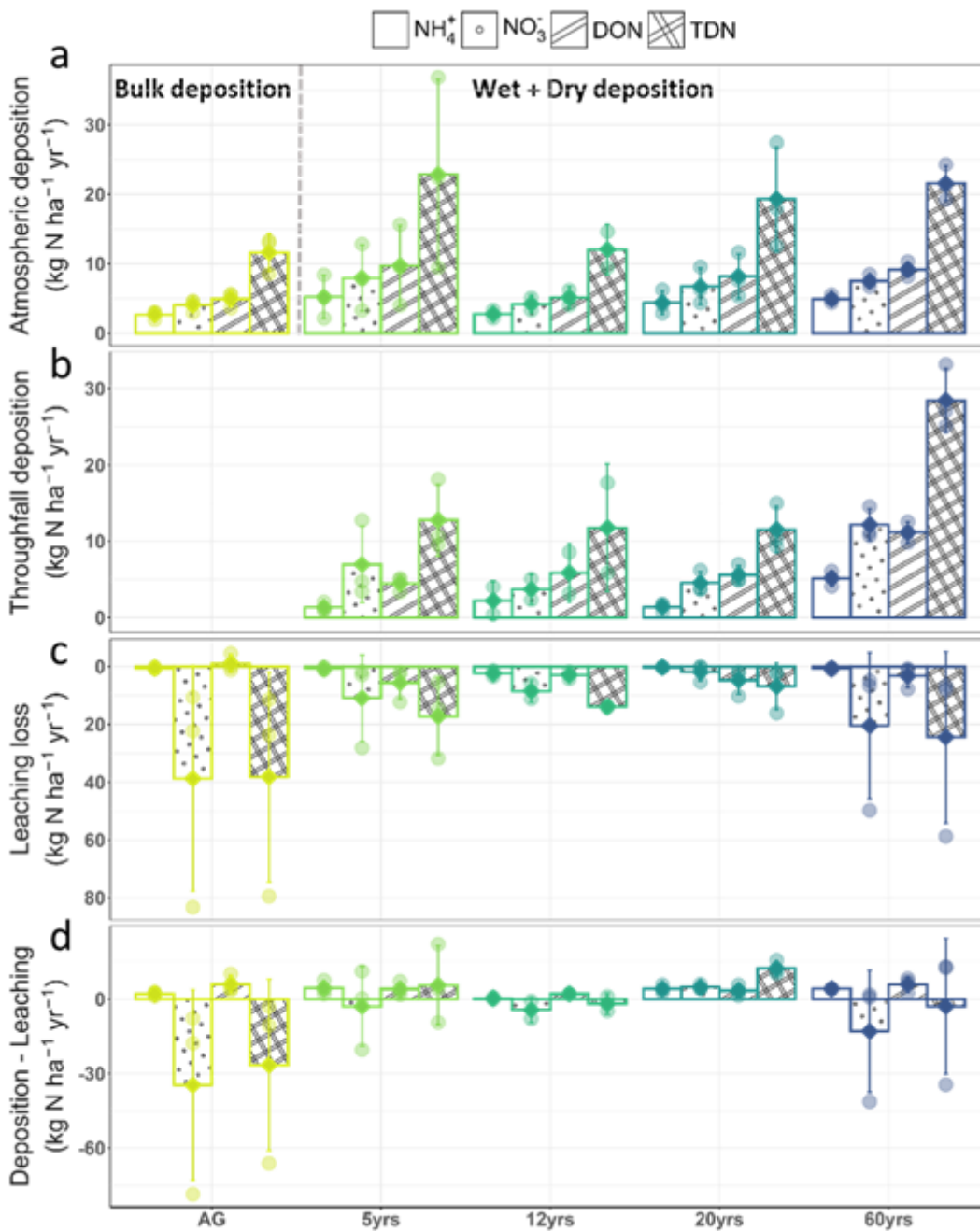


Figure 2

Ammonium (NH_4^+), nitrate (NO_3^-), dissolved organic carbon (DON) and total dissolved nitrogen (TDN) input, output and partial deposition - leaching balance along the studied secondary succession gradient; a) bulk (i.e. wet) and total atmospheric (i.e. wet + dry) deposition ($\text{kg N ha}^{-1} \text{ yr}^{-1}$), b) throughfall deposition (wet + dry + canopy leaching) deposition ($\text{kg N ha}^{-1} \text{ yr}^{-1}$), c) leaching loss at 80 cm depth ($\text{kg N ha}^{-1} \text{ yr}^{-1}$), d) partial deposition leaching budget ($\text{kg N ha}^{-1} \text{ yr}^{-1}$). AG, 5yrs, 12yrs, 20yrs and 60yrs indicate the agricultural sites and 5, 12, 20 and 60 years-old secondary forests. The bars and diamond shaped points represent successional stages mean; circle points are plot level data and error bars are standard deviations.

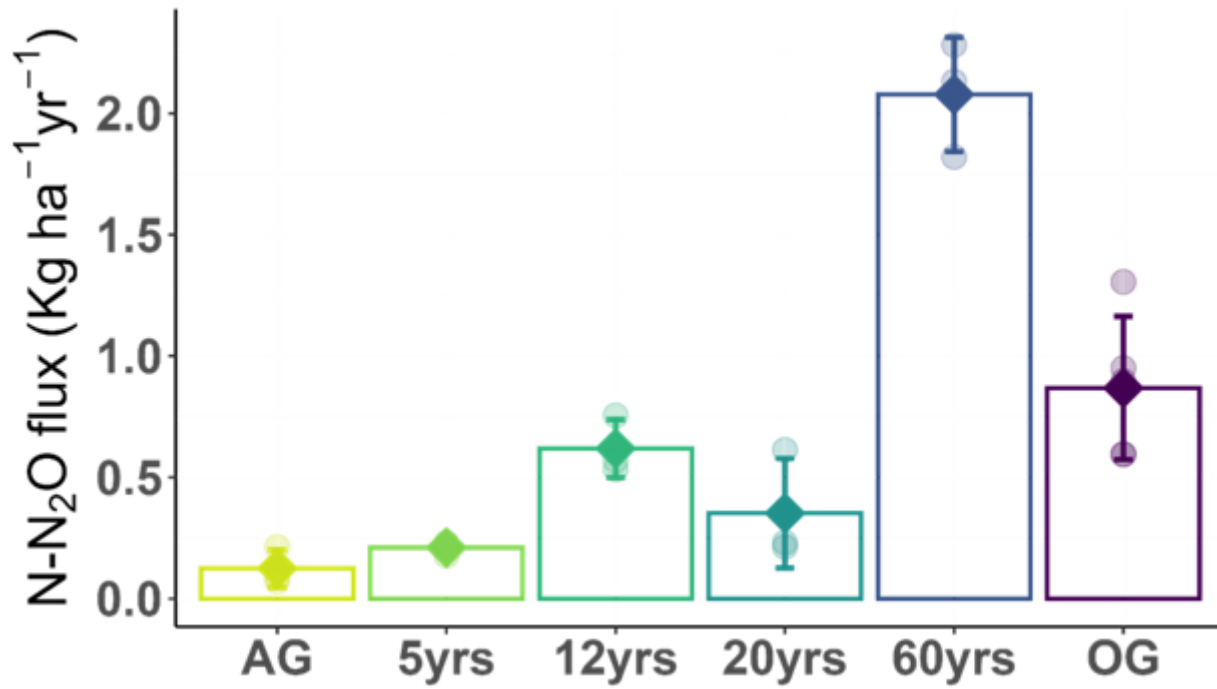


Figure 3

Soil N₂O emission (kg N ha⁻¹ yr⁻¹) along secondary forest succession in the Congo basin. AG, 5yrs, 12yrs, 20yrs, 60yrs and OG stand respectively for the agricultural sites, 5, 12, 20, 60 years-old secondary forests and old growth forest. The bars and diamond shaped points represent successional stages mean; circle points are plot level data and error bars are standard deviations.

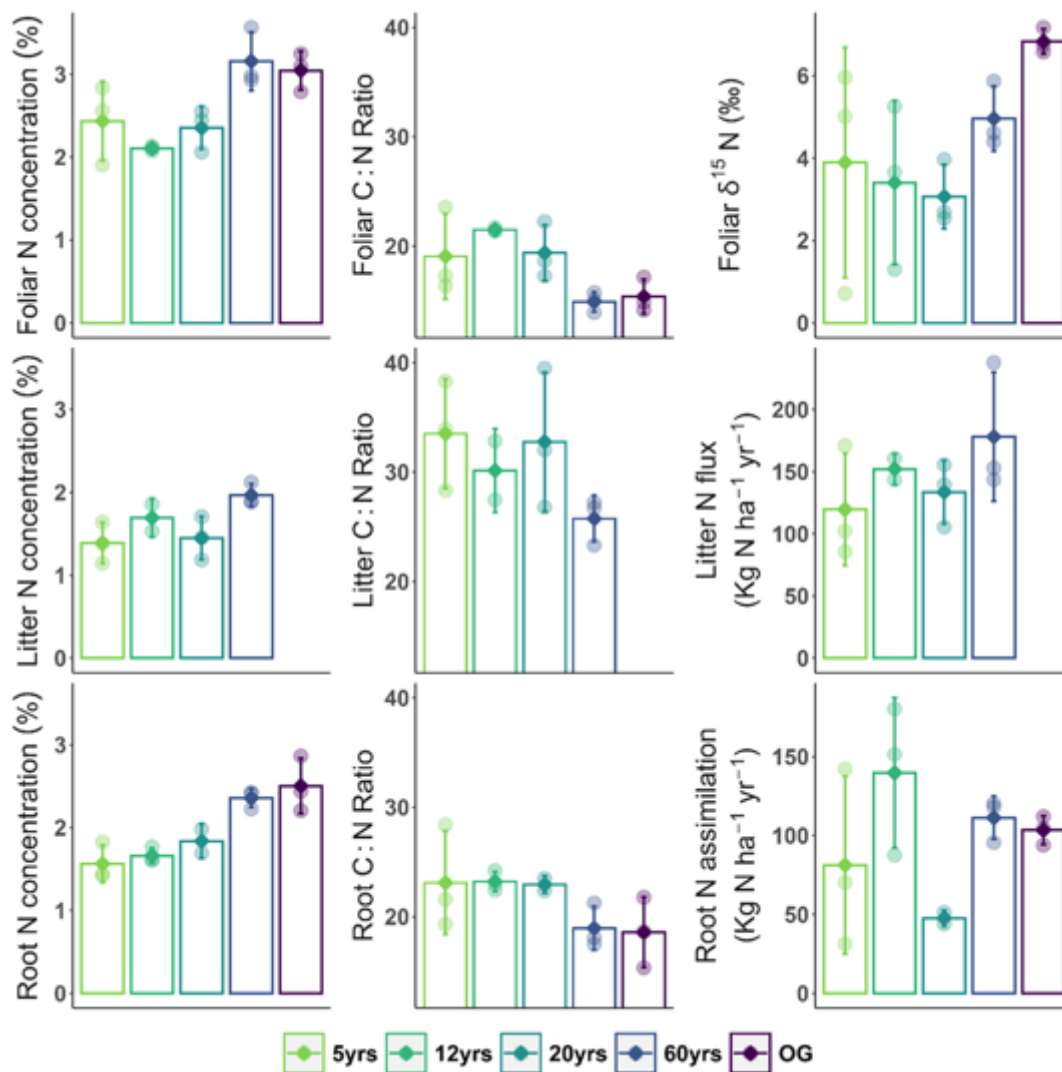


Figure 4

Variation of vegetation tissue N metrics along secondary succession including foliar, litter and root C:N ratios; foliar, litter and root N concentration (%), litter and root internal N recycling ($\text{kg N ha}^{-1} \text{ yr}^{-1}$) and foliar $\delta^{15}\text{N}$ (‰); 5yrs, 12yrs, 20yrs, 60yrs and OG stand respectively for 5, 12, 20 and 60 years-old secondary forests and the old growth forest. The bars and diamond shaped points represent successional stages mean; circle points are plot level data and error bars are standard deviations.

Supplementary Files

This is a list of supplementary files associated with this preprint. Click to download.

- [Makeleleetal.SupplementaryMaterial.docx](#)